Sonoluminescing Air Bubbles Rectify Argon

Detlef Lohse,[1] Michael P. Brenner,[2] Todd F. Dupont,[3] Sascha Hilgenfeldt,[1] and Blaine Johnston[4]

[1]*Fachbereich Physik der Universität Marburg, Renthof 6, 35032 Marburg, Germany*
[2]*Department of Mathematics, Massachusetts Institute of Technology, Cambridge, Massachusetts 02139*
[3]*Department of Computer Science, University of Chicago, Chicago, Illinois 60637*
[4]*Department of Physics, University of Chicago, Chicago, Illinois 60637*

The dynamics of single bubble sonoluminescence (SBSL) strongly depends on the percentage of inert gas within the bubble. We propose a theory for this dependence, based on a combination of principles from sonochemistry and hydrodynamic stability. The nitrogen and oxygen dissociation and subsequent reaction to water soluble gases implies that strongly forced air bubbles eventually consist of pure argon. Thus it is the partial argon (or any other inert gas) pressure which is relevant for stability. The theory provides quantitative explanations for many aspects of SBSL. [S0031-9007(97)02404-6]

PACS numbers: 78.60.Mq, 42.65.Re, 43.25.+y, 82.40.We

Recent experiments [1] revealed that a single gas bubble levitated in a strong acoustic field $P(t) = P_a \cos \omega t$ can emit picosecond bursts of light, a phenomenon called single bubble sonoluminescence (SBSL). The phase and intensity of the light can be stable for hours. SBSL shows a sensitive dependence on the forcing pressure, the concentration of the dissolved gas, and the liquid temperature, among other parameters.

Particularly puzzling is the dependence on the type of the gas dissolved in the liquid. Hiller *et al.* [2] demonstrated that stable SBSL does not occur with pure nitrogen, oxygen, or nitrogen-oxygen mixtures. But a critical concentration of argon gives stable SBSL. This paper presents an explanation for this dependence on the type of gas, based on combining principles from sonochemistry [3,4] with hydrodynamic stability [5].

An important clue comes from experiments [6,7] showing that the range of gas concentrations for stable SBSL in pure argon bubbles differs from that for air bubbles by 2 orders of magnitude. Stable SBSL in argon requires strong degassing of the liquid down to the tiny gas pressure $p_\infty = 0.004P_0$, which by Henry's law corresponds to a concentration $c_\infty = 0.004c_0$, where $P_0 = 1$ atm and c_0 is the saturation concentration. In contrast to argon, SBSL with air only requires degassing down to $p_\infty/P_0 = 0.1-0.4$ [6,8]. Löfstedt *et al.* [7] estimated that diffusive equilibrium of the bubble with the surrounding dissolved gas requires $p_\infty/P_0 \sim 10^{-3}$, suggesting agreement with the experiments for argon, but not air. Indeed, detailed hydrodynamic stability calculations [5] show quantitative agreement with argon data. The strong discrepancy led Löfstedt *et al.* to the conjecture that there is an "as yet unidentified mass ejection mechanism" in air bubbles which "is the key to SL in a single bubble."

We suggest that this mechanism is chemical. The importance of chemical reactions has long been recognized in multibubble sonoluminescence (MBSL) in transient cavitation clouds [4,9], since the pioneering work of

Schultes and Gohr [3] found that aqueous solutions of nitrogen produced nitric and nitrous acids when subjected to ultrasound. High temperatures generated by the bubble collapse are beyond the dissociation temperature of oxygen and nitrogen ($\approx$9000 K), leading to the formation of O and N radicals which react with the H and O radicals formed from the dissociation of water vapor. Rearrangement of the radicals will lead to the formation of NO, OH, NH, which eventually dissolve in water to form HNO_2 and HNO_3, among other products.

Based on fits of SBSL spectra [10,11] and hydrodynamic calculations [12,13], it is well accepted that internal bubble temperatures in SBSL are even higher than in MBSL. Therefore, the same reactions as in MBSL will occur. The reaction products (NO_2, NO, ...) are pressed into the surrounding liquid, and are not recollected during the next bubble cycle, since their solubility in water is enormous. This chemical process deprives the gas in the bubble of its reactive components. Small amounts of N_2 and O_2 that diffuse into the bubble during the expansion react, and their dissociation products are expelled back into the surrounding liquids at the bubble collapse. The only gases that can remain within a SBSL bubble over many bubble cycles are those which at high temperatures do not react with the liquid vapor, i.e., inert gases. Hence, when air is dissolved in water, a strongly forced bubble is almost completely filled with argon. This argon rectification happens in SBSL but not in MBSL because it requires bubble stability over many oscillation cycles.

In the following, we first present qualitative consequences of argon rectification, demonstrating that even at a crude level it resolves central problems of bubble stability. Then we proceed to make the argument more precise through quantitative calculation.

If the bubble is filled essentially with argon, the hydrodynamic stability of the bubble is determined by the *partial* pressure of argon $p_\infty^{Ar} = \xi_l p_\infty$, where ξ_l ($= 0.01$ for air) is the argon ratio of gas dissolved in the

liquid. This fact immediately resolves the hundredfold difference between the amount of degassing necessary for air versus argon: As mentioned above, hydrodynamic stability calculations [5] demonstrate that stable sonoluminescence for argon bubbles exists between $p_{lower} < p_\infty^{Ar}/P_0 < p_{upper}$, with $[p_{lower}, p_{upper}]$ depending on the forcing pressure P_a (Fig. 1). For example, at $P_a = 1.3$ atm, $[p_{lower}, p_{upper}] \approx [0.002, 0.004]$. Since the stability window for air bubbles is set by the partial pressure of argon $p_\infty^{Ar} = 0.01 p_\infty$, the total pressure of the air mixture must be in the range $[100 p_{lower}, 100 p_{upper}]$ for stable SL. At $P_a = 1.3$ atm, this corresponds to $0.2 < p_\infty/P_0 < 0.4$, in good agreement with experiments. One reason that air with its 1% argon is a particularly friendly gas for SL experiments is that this amount of degassing is easily achieved.

At this simple level, the theory makes several other explicit predictions: When varying the percentage of argon in N_2-Ar mixtures the range of p_∞/P_0 where SL is stable should vary like $p_{lower}/\xi_l < p_\infty/P_0 < p_{upper}/\xi_l$, with the upper threshold, the lower threshold, and the range increasing with decreasing argon fraction ξ_l. Another consequence is that there is an argon ratio ($\xi_l \approx 0.003$ at $P_a = 1.3$ atm) for which stable SL should be possible *without degassing*. We caution that to achieve this it is necessary to rid the liquid of impurities to avoid spontaneous cavitation.

Also the different character of the transition to SBSL observed in air bubbles and in argon bubbles can be
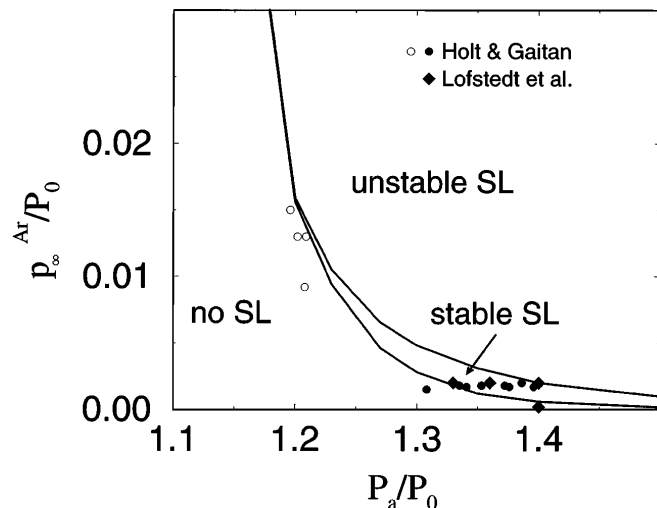
FIG. 1. Phase diagram for pure argon bubbles in the p_∞^{Ar}/P_0 versus P_a/P_0 parameter space, from [5], but now with experimental data included. Stable SL is only possible in a very small window of argon concentration. The experimental data points refer to observed stable SL (filled symbols) or stable non-SL bubbles (open symbols) and are extracted (using the present theory) from Refs. [7] (diamonds) and [18] (circles) and show good agreement with the theory. This theoretical figure compares well with the experimental result; cf. Fig. 1(c) of [18].

explained by our theory: Hiller *et al.* [2] showed that for pure argon bubbles, the bubble mass increases smoothly and monotonically upon increasing the forcing pressure. In contrast Barber *et al.* [6] found that the transition to SBSL in air bubbles causes an abrupt decrease in the bubble mass. The difference between these two experiments is the presence or absence of sonochemical reactions: In air bubbles an abrupt behavior occurs when the forcing pressure corresponds to the onset of the dissociation reaction. Below this threshold, the bubble contains air, and the ambient radius is determined by the diffusive stability of the mixture. Above the transition, when the molecular gases dissociate, the equilibrium radius is set by diffusive stability of pure argon bubbles resulting in a much different ambient radius [5]. The transition towards SL is smooth for pure argon because a dissociation mechanism is absent.

We now turn to a quantitative calculation of hydrodynamic stability for gas mixtures with chemical reactions. The bubble radius $R(t)$ is well described by the Rayleigh-Plesset equation [12], which we take to have the same form and parameters as in our earlier work [5]. The internal bubble pressure $p(t)$ is assumed to obey a van der Waals equation of state. Now consider a bubble in water containing a mixture of a reactive gas (taken to be N_2) and an inert gas, Ar. The total number of moles of gas in the bubble is $N_{tot} = 4\pi R_0^3 P_0/3G\Theta_0 = N_{N_2} + N_{Ar}$, where $\Theta_0 = 273$ K is the normal temperature and $G = 8.3143$ J/(mol K) is the gas constant. The argon fraction *in* the bubble is $\xi_b = N_{Ar}/N_{tot}$, that of nitrogen $1 - \xi_b = N_{N_2}/N_{tot}$. If $c^{Ar}(r, t)$ and $c^{N_2}(r, t)$ are the mass-per-volume concentration fields of Ar and N_2 in the liquid, respectively, the rate of change of the number of molecules of N_2 and Ar in the bubble is given by

$$\dot{N}_{Ar} = \frac{4\pi R^2 D_{Ar}}{\mu_{Ar}} \partial_r c^{Ar}|_{r=R}, \tag{1}$$

$$\dot{N}_{N_2} = \frac{4\pi R^2 D_{N_2}}{\mu_{N_2}} \partial_r c^{N_2}|_{r=R} - A N_{N_2} \exp\left(-\frac{\Theta^*}{\Theta}\right). \tag{2}$$

Here, D_{Ar}, D_{N_2}, μ_{Ar}, and μ_{N_2} are the respective diffusion constants and molecular masses. The concentration fields obey an advection diffusion equation, whose boundary conditions are set by the external concentrations $c^\alpha(\infty, t) = c_\infty^\alpha = p_\infty^\alpha c_0^\alpha/P_0$ (Henry's law) and by the partial gas pressures $p^\alpha(t)$ in the bubble $c^\alpha(R(t), t) = p^\alpha(R(t))c_0^\alpha/P_0$, $\alpha =$ Ar, N_2. The second term in (2) represents the bubble's nitrogen loss by chemical reactions. The reaction rate depends on the temperature $\Theta(t)$ in the bubble. For simplicity, we assume that the reactions follow an Arrhenius law, with empirical parameters appropriate for nitrogen dissociation (Ref. [14]): $A = 6 \times 10^{19}(\Theta_0/\Theta)^{2.5}(\rho_0/\mu_{N_2})(R_0/R)^3$ cm^3/(mol s) giving the time scale of the reaction; $\Theta^* = 113\,000$ K is the activation temperature and ρ_0 the equilibrium gas density. This reaction law is rather crude, as it neglects backward

reactions as well as the kinetics of the expulsion of reaction products; however, it is sufficient for this demonstrative calculation.

The diffusive mass flux into the bubble can be calculated explicitly using the fact that the diffusive time scale is much slower than the bubble oscillation period T [5,7,15,16]. This reduces the diffusional problem to the calculation of weighted averages of the form $\langle f \rangle_i = \int_0^T f(t) R^i(t)\, dt / \int_0^T R^i(t)\, dt$, with the mass flux proportional to $p_\infty - \langle p \rangle_4$ for a pure gas [15]. Applying the same approximation to Eqs. (1) and (2) gives

$$\frac{\Delta N_{Ar}}{T} \approx \frac{4\pi R_m D_{Ar} c_0^{Ar}}{\mu_{Ar} P_0} (p_\infty^{Ar} - \xi_b \langle p \rangle_4), \qquad (3)$$

$$\frac{\Delta N_{N_2}}{T} \approx \frac{4\pi R_m D_{N_2} c_0^{N_2}}{\mu_{N_2} P_0} (p_\infty^{N_2} - (1 - \xi_b) \langle p \rangle_4)$$
$$- N_{N_2} \langle A \exp(-\Theta^*/\Theta) \rangle_0, \qquad (4)$$

$R_m = \max R(t)$. To close the equations, we need a model for the temperature dependence $\Theta(t)$. The actual temperature dependence is determined by complicated nonlinear processes operating during the collapse. As a simple model, we take the temperature to be uniform within the bubble, and use the polytropic law $\Theta(t) = \Theta_0 ((R_0^3 - h^3)/[R^3(t) - h^3])^{\gamma-1}$ with h the van der Waals hard core radius and γ the polytropic exponent. The value of γ depends on the rate of heat transport from the bubble, which is characterized by the Péclet number $Pe = \dot{R} R_0^2 / R\kappa$, where κ is the thermal diffusivity of the gas. During the bubble expansion, $Pe \ll 1$ (isothermal behavior, $\gamma = 1$); during the bubble collapse, $Pe \gg 1$ (adiabatic compression, $\gamma = 5/3$). Since both of these regimes occur during a single bubble cycle, it is necessary to use a model which interpolates between them. For definiteness, we follow Prosperetti [17] and use his calculated $\gamma(Pe)$. We emphasize that although this treatment of the chemical reactions is crude, the central results discussed below are robust.

With these approximations, the equilibrium states (satisfying $\Delta N_{Ar} = \Delta N_{N_2} = 0$) can be computed as a function of (N_{Ar}, N_{N_2}), or equivalently as a function of (ξ_b, R_0). Figure 2 shows the equilibrium radii R_0^* in the R_0-P_a plane for air at $p_\infty/P_0 = 0.2$. For small forcing the temperatures are not high enough to initiate chemical reactions, so that the equilibrium curve corresponds to the classical prediction by Eller and Flynn [16] for this gas concentration. This equilibrium is unstable: The bubble either shrinks or grows by rectified diffusion; experiments [6,8,13] show that a growing bubble eventually runs into a shape instability where microbubbles pinch off and make the bubble dance because of the recoil [5]. In the opposite limit of high forcing (curve C), the reactions burn off all the N_2, so that the bubble contains pure argon; this equilibrium corresponds to the (stable) Eller-Flynn equilibrium at the argon partial pressure $p_\infty^{Ar}/P_0 = 0.01 p_\infty/P_0 = 0.002$.
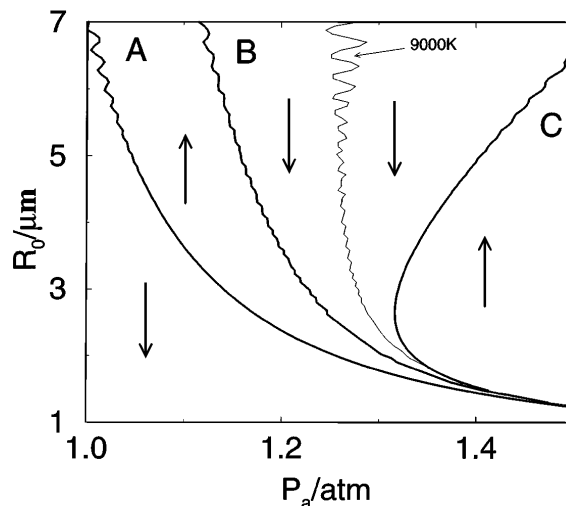
FIG. 2. Phase diagram for air at $p_\infty/P_0 = 0.2$ in the R_0-P_a space. The arrows denote whether the ambient radius grows or shrinks at this parameter value. Curve A denotes the equilibrium for an air bubble; on curve C the bubble only contains argon. The intermediate curve B necessarily exists because of the topology of the diagram, and represents an additional stable equilibrium. Above and right of the thin line, the gas temperature exceeds the nitrogen dissociation threshold of about 9000 K.

Figure 2 displays a regime of shrinking bubbles at high forcing pressures (left of curve C) and an adjacent region of growing bubbles (right of curve A). This necessitates the existence of an additional equilibrium at intermediate forcing pressures, curve B in Fig. 2, for which growth by rectified diffusion and loss by reactions balance. This additional equilibrium occurs close to the point of nitrogen dissociation, and turns out to be stable; the argon fraction ξ_b^* for this equilibrium is slightly larger than the fraction ξ_l in the liquid (for not too strong forcing). The only feature of Fig. 2 that depends on the details of temperature and chemical reactions is the exact position of the nitrogen dissociation threshold and thus the exact position of curve B.

Figure 3 plots the equilibrium composition ξ_b^*, given by $\Delta N_{Ar}/\Delta N_{N_2} = \xi_b^*/(1 - \xi_b^*)$. Weakly forced bubbles have $\xi_b^* \approx \xi_l$, thus $p_\infty/P_0 = 0.20$ is relevant for stability. Strongly forced bubbles have $\xi_b^* \approx 1 \gg \xi_l$, thus $p_\infty^{Ar}/P_0 = 0.002$ is the relevant quantity. The transition between these regimes is abrupt, and occurs when the bubble temperature surpasses the dissociation temperature (≈ 9000 K for N_2).

What happens for even lower argon concentration $\xi_l < 0.01$ in the dissolved gas? For these low concentrations the equilibria curves A and B hardly depend on ξ_l. This holds even in the limit $\xi_l \to 0$ of pure nitrogen bubbles. Therefore, our theory predicts that there is a parameter regime of forcing pressures where stable N_2 bubbles exist. The equilibrium curve C, of course, does depend on ξ_l and for decreasing argon concentration $p_\infty^{Ar} = \xi_l p_\infty$ it moves further and further to the right, allowing diffusively stable
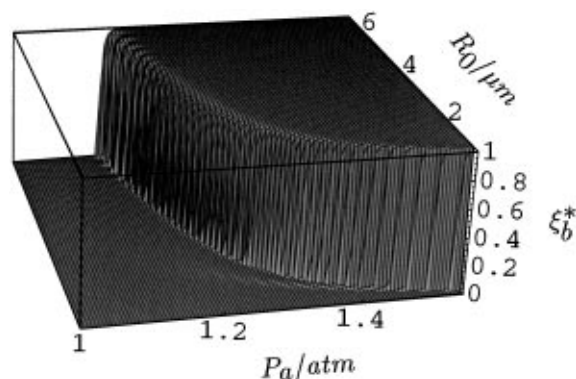
FIG. 3. The equilibrium fraction ξ_b^* of argon in the bubble as a function of P_a and R_0.

SL bubbles only for larger and larger forcing. Finally, spherical instability will destroy these bubbles [5].

Having calculated the above phase diagrams, we come back to a comparison to experiments. For an air bubble, upon increasing the forcing pressure, the bubble will eventually encounter the stable equilibrium curve B; tracking curve B on further increasing the forcing pressure leads to an abrupt decrease in the bubble size. The experimentally observed abrupt decrease in the ambient radius reflects the sharpness of the slope of curve B. Eventually, at high enough forcing pressure, the bubble will track curve C, the ambient radius now increasing with forcing pressure.

The most extensive experimental evidence in support of these calculations is Holt and Gaitan's [18] recent detailed measurement of phase diagrams in the R_0-P_a plane. At low forcing pressure, they observe bubble equilibria in agreement with classical calculations using the pressure head ($p_\infty/P_0 = 0.2$) applied in the experiments. At very high forcing pressure, the bubble equilibria agree with classical calculations, but only when $p_\infty^{Ar}/P_0 = 0.002$ is used in the equations. Between these two regimes, Holt and Gaitan find the additional stable equilibria (curve B) of nonsonoluminescing bubbles and an adjacent region (at $P_a \sim 1.2-1.3$ atm) where bubbles dissolve, very similar to that between curves B and C in Fig. 2. In addition, Holt and Gaitan also find the size of the dissolution region decreases with increasing p_∞/P_0, which also follows directly from the theory.

To summarize, the combination of the principles of sonochemistry and hydrodynamic stability leads to a consistent picture of the stability of sonoluminescing bubbles for gas mixtures and makes many predictions. Our central statement is that it is only p_∞^{Ar}/P_0 which is relevant for SL stability in the high P_a regime. We included all available experimental data (with sufficient information on P_a and p_∞) in our theoretical phase diagram [5] Fig. 1 to demonstrate the good agreement. Finally, we suggest to measure the concentrations of the reaction products as a function of time for SBSL, as already done in MBSL [19]. Nitrous acid production

would lead to a decrease in pH. For an estimate of an upper bound to the production rate we assume that reactions at the collapse burn off all the nitrogen that diffuses into the bubble during its expansion. This amount of gas is estimated in Ref. [7] as $\Delta N_{N_2} = 2\pi D_{N_2} c_\infty^{N_2} R_m T / \mu_{N_2}$ per cycle. With typical values of $R_m = 10R_0$ for the maximal radius, $R_0 = 5$ μm, $D_{N_2} = 2 \times 10^{-9}$ m^2/s, $c_\infty^{N_2} \approx 0.20 c_0^{N_2}$, $c_0^{N_2} = 0.02$ kg/m^3, and $T = 37$ μs one obtains $\Delta N_{N_2} \approx 3 \times 10^{-18}$ mol per cycle or $\sim 3 \times 10^{-10}$ mol of N$_2$ per hour converted to reaction products. This results in a small but detectable pH decrease.

[1] For recent reviews and further references, see S. J. Putterman, Sci. Am. **272**, No. 2, 32 (1995); L. A. Crum, Phys. Today **47**, No. 9, 22 (1994).

[2] R. Hiller, K. Weninger, S. J. Putterman, and B. P. Barber, Science **266**, 248 (1994).

[3] H. Schultes and H. Gohr, Angew. Chem. **49**, 420 (1936).

[4] *Sonoluminescence in Ultrasound: Its Chemical, Physical and Biological Effects,* edited by K. Suslick (VCH, Weinheim, 1988).

[5] S. Hilgenfeldt, D. Lohse, and M. P. Brenner, Phys. Fluids **8**, 2808 (1996); M. Brenner, D. Lohse, and T. Dupont, Phys. Rev. Lett. **75**, 954 (1995); M. Brenner, D. Lohse, D. Oxtoby, and T. Dupont, Phys. Rev. Lett. **76**, 1158 (1996).

[6] B. P. Barber, K. Weninger, R. Löfstedt, and S. J. Putterman, Phys. Rev. Lett. **74**, 5276 (1995).

[7] R. Löfstedt, K. Weninger, S. J. Putterman, and B. P. Barber, Phys. Rev. E **51**, 4400 (1995).

[8] D. F. Gaitan, Ph.D. thesis, The University of Mississippi, 1990.

[9] For reviews and further references, see M. A. Margulis, Ultrasonics **23**, 157 (1985); K. S. Suslick, Science **247**, 1439 (1990).

[10] L. Bernstein and M. Zakin, J. Phys. Chem. **99**, 14 619 (1995).

[11] R. Hiller, S. J. Putterman, and B. P. Barber, Phys. Rev. Lett. **69**, 1182 (1992).

[12] R. Löfstedt, B. P. Barber, and S. J. Putterman, Phys. Fluids A **5**, 2911 (1993).

[13] B. P. Barber *et al.,* Phys. Rev. Lett. **72**, 1380 (1994).

[14] L. Bernstein, M. Zakin, E. Flint, and K. Suslick, J. Phys. Chem. **100**, 6612 (1996).

[15] M. M. Fyrillas and A. J. Szeri, J. Fluid Mech. **277**, 381 (1994).

[16] A. Eller, J. Acoust. Soc. Am. **46**, 1246 (1969); A. Eller and H. G. Flynn, J. Acoust. Soc. Am. **37**, 493 (1964).

[17] A. Prosperetti, J. Acoust. Soc. Am. **61**, 17 (1977).

[18] G. Holt and F. Gaitan, Phys. Rev. Lett. **77**, 3791 (1996).

[19] E. Hart, C. H. Fischer, and A. Henglein, J. Phys. Chem. **91**, 4166 (1987).